HHS Public Access

Author manuscript

Neuroimage. Author manuscript; available in PMC 2016 April 15.

Published in final edited form as:

Neuroimage. 2015 April 15; 110: 39–47. doi:10.1016/j.neuroimage.2015.01.046.

Does acute caffeine ingestion alter brain metabolism in young adults?

Feng Xu[a,b,c], **Peiying Liu**[a,b,d], **James J. Pekar**[b,c], and **Hanzhang Lu**[a,b,d]

[a]Advanced Imaging Research Center, University of Texas Southwestern Medical Center, 5323 Harry Hines Blvd, Dallas, TX 75390, United States

[b]The Russell H. Morgan Department of Radiology & Radiological Science, Johns Hopkins University, 601 North Caroline Street, MD 21287, United States

[c]F. M Kirby Center for Functional Brain imaging, Kennedy Krieger Institute, 707 N Broadway, Baltimore, MD, 21205, United States

[d]Department of Psychiatry, University of Texas Southwestern Medical Center, 5323 Harry Hines Blvd, Dallas, TX 75390, United States

Abstract

Caffeine, as the most commonly used stimulant drug, improves vigilance and, in some cases, cognition. However, the exact effect of caffeine on brain activity has not been fully elucidated. Because caffeine has a pronounced vascular effect which is independent of any neural effects, many hemodynamics-based methods such as fMRI cannot be readily applied without a proper calibration. The scope of the present work is two-fold. In Study 1, we used a recently developed MRI technique to examine the time-dependent changes in whole-brain cerebral metabolic rate of oxygen ($CMRO_2$) following the ingestion of 200mg caffeine. It was found that, despite a pronounced decrease in CBF ($p<0.001$), global $CMRO_2$ did not change significantly. Instead, the oxygen extraction fraction (OEF) was significantly elevated ($p=0.002$) to fully compensate for the reduced blood supply. Using the whole-brain finding as a reference, we aim to investigate whether there are any regional differences in the brain's response to caffeine. Therefore, in Study 2, we examined regional heterogeneities in CBF changes following the same amount of caffeine ingestion. We found that posterior brain regions such as posterior cingulate cortex and superior temporal regions manifested a slower CBF reduction, whereas anterior brain regions including dorsolateral prefrontal cortex and medial frontal cortex showed a faster rate of decline. These findings have a few possible explanations. One is that caffeine may result in a region-dependent increase or decrease in brain activity, resulting in an unaltered average brain metabolic rate. The

Corresponding Author: Hanzhang Lu, Ph.D., Advanced Imaging Research Center, UT Southwestern Medical Center, 5323 Harry Hines Blvd., Dallas, TX 75390, hanzhang.lu@gmail.com, Tel: 1-214-645-2761, Fax: 1-214-645-2744.

Disclosure/Conflict of interest

The authors declare no conflict of interest.

other is that caffeine's effect on vasculature may be region-specific. Plausibility of these explanations is discussed in the context of spatial distribution of the adenosine receptors.

Keywords

caffeine; cerebral metabolic rate of oxygen; cerebral blood flow; cerebral venous oxygenation; oxygen extraction fraction; TRUST MRI

Introduction

Caffeine is the most widely used stimulant drug in the western countries. The primary psychological effects of caffeine are mitigation of drowsiness and improvement in vigilance (Magill et al., 2003). However, the impact of caffeine ingestion on brain physiology is not fully characterized, especially in humans (Chen and Parrish, 2009; Griffeth et al., 2011; Laurienti et al., 2002; Liu et al., 2004; Wong et al., 2012). Caffeine acts through its complex effects on a number of neurotransmission systems such as dopamine, acetylcholine, serotonin, and, in high doses, norepinephrine (Berkowitz and Spector, 1971; Berkowitz et al., 1970; Ferre, 2010; Nehlig et al., 1992). However, the most prominent and widely studied effect of caffeine in the brain is its role as an antagonist of the inhibitory neurotransmitter, adenosine. Adenosine and some subtypes of its receptors, e.g. A_1 adenosine receptor, are found throughout the brain, and they reduce synaptic vesicle release in the presynaptic terminal among other functions (Fredholm et al., 1999; Goodman and Synder, 1982; Premont et al., 1979). Therefore, it is reasonable to hypothesize that blocking of the adenosine neurotransmission by caffeine may increase neural activity and whole-brain metabolic rate.

While conceptually simple, this question has not been thoroughly examined, mainly due to a scarcity of measurement techniques applicable in humans. Positron emission tomography (PET) has been used for the measurement of brain metabolism in clinical studies. However, there have been few reports on its use in studies of caffeine effect on the brain, possibly because of several factors such as concerns associated with repeated radiation exposure, the complexity in dynamic sampling of arterial blood, and the need of an onsite cyclotron in the case of oxygen metabolism measurement (Chen et al., 2009; Di et al., 2013; Park et al., 2014). Recently, we have developed a novel method that can provide a non-invasive (no exogenous tracer nor agent), rapid (<5 min), and reliable (coefficient of variation less than 4%) measurement of global cerebral metabolic rate of oxygen ($CMRO_2$) on a standard 3T MRI (Liu et al., 2013; Xu et al., 2009; Xu et al., 2011). The present study applies this new method to examine the effect of caffeine ingestion on whole-brain oxygen metabolism in healthy humans.

Given that certain subtypes of the adenosine receptor, e.g. A_{2A}, are heterogeneously distributed in the brain (Fredholm et al., 1999; Mishina et al., 2007; Pelligrino et al., 2010), we further investigate regional differences in the brain's physiological response to caffeine. We measured cerebral blood flow (CBF) which reflects a combined contribution of a direct effect of caffeine on cerebrovasculature and an indirect effect through potential modulations on neural activity and brain metabolism (Alsop et al., 2014; Donahue et al., 2006; Kety and

Schmidt, 1948). We reason that, if a regional heterogeneity can be identified, it would indicate that either the direct vasoconstriction effect is region-dependent or that neural response to caffeine is different across brain regions.

The present work therefore contains two sets of studies. In Study 1, we used a global $CMRO_2$ technique to examine dynamic changes in brain oxygen metabolism. Ten healthy human subjects took a 200 mg caffeine tablet and underwent a continuous MRI scan of 40 minutes, during which whole-brain $CMRO_2$ was measured every 4.5 minutes. Another ten subjects served as controls and underwent the same MRI session but did not take the caffeine tablet. In Study 2, ten healthy human subjects took a 200 mg caffeine tablet and underwent a continuous MRI scan of 40 minutes, during which voxel-by-voxel CBF maps were collected using Arterial-Spin-Labeling (ASL) MRI.

Materials and Methods

General

MRI scans were performed on a 3 Tesla MRI system (Philips Healthcare, Best, The Netherlands). A body coil was used for radiofrequency transmission and a 32-channel head coil was used for receiving. Foam padding was used to stabilize the subject's head and to minimize motion. The study protocol was approved by the Institutional Review Board of the University of Texas Southwestern Medical Center. Each subject gave informed written consent before participating in the study. A total of thirty healthy subjects (27±4 years old, 15 males, 15 females, 20 for Study 1 and 10 for Study 2) were recruited from the university campus through flyers. The participants were carefully screened and did not report neurological, psychiatric, endocrine disorders or diabetes according to self-completed questionnaires. The participants did not have MR contraindications such as metal implants, pacemaker, neurostimulator, body piercings, or claustrophobia. The participants were not regular coffee drinkers and were asked to avoid any type of caffeine beverages for a week before the experiment.

Study 1: The effect of caffeine ingestion on whole-brain $CMRO_2$

Experimental procedures—Ten subjects (28±5 years old, range from 22 to 35, 5 males and 5 females) participated in the caffeine experiment. Figure 1 illustrates the procedures at the research facility. The first time point of $CMRO_2$ measurement was obtained by 7.4±0.3 (mean ± standard error) minutes after taking the tablet, which is considered baseline values given the relatively small change in blood caffeine level at this early time point (Kamimori et al., 2002). We employed this procedure instead of the repositioning scheme (i.e. remove from and enter the scanner again) so that data fluctuation due to repositioning inconsistency is minimized and this allows us to perform continuous measurements without time gap. Arterial oxygen saturation (Y_a) was measured at finger with pulse oximetry (Invivo, Gainesville, FL).

Another ten subjects (27±4 years old, range from 23 to 30, 6 males and 4 females) participated in the control experiment. The purpose of the control experiment was to test the possibility that the physiologic changes observed in the caffeine study was due to non-

caffeine related effects such as drowsiness or fatigue caused by lying inside scanner for 40 minutes. The procedures for the control experiment were identical to the caffeine ingestion experiment except that the participant did not take the caffeine tablet (Figure 1).

Theory for the measurement of Global $CMRO_2$—Our approach to estimate $CMRO_2$ was based on the Fick principle (Jain et al., 2010; Kety and Schmidt, 1948; Rodgers et al., 2013; Xu et al., 2009), by which $CMRO_2$ can be calculated using:

$$CMRO_2 = CBF \cdot (Y_a - Y_v) \cdot C_h \quad [1]$$

where $CMRO_2$ is in units of μmol/100g/min, CBF is in units of ml/100g/min, Y_a and Y_v (in percentage, %) are oxygenation in arterial and venous blood, respectively, and C_h represents the oxygen carrying capability of hemoglobin and is 8.97 μmol O_2/ml blood at typical Hct of 0.44 (Guyton and Hall, 2005). The actual value of C_h used in our calculation was subject-specific based on the individually determined Hct.

Among the parameters needed to compute $CMRO_2$, the most challenging task has been the measurement of Y_v. We have recently developed and validated a technique, T_2-Relaxation-Under-Spin-Tagging (TRUST) MRI, to estimate Y_v in the sagittal sinus (Lu and Ge, 2008; Lu et al., 2012). This technique was found to be highly reproducible and can be conducted within 1.2 minutes (Liu et al., 2013; Xu et al., 2011). TRUST MRI is based on the principle that blood oxygenation has a known relationship with blood T_2 (Golay et al., 2001; Oja et al., 1999; Silvennoinen et al., 2003). This technique uses spin tagging method to isolate pure venous blood signal from surrounding tissue and measures T_2 value of the blood, which can be converted to Y_v via a calibration plot (Lu et al., 2012). By assuming that Y_v measured in the sagittal sinus is a close approximation of the whole-brain Y_v, we can obtain the global Y_v with this method. The term of $(Y_a - Y_v)/Y_a$ is further defined as oxygen extraction fraction (OEF).

Global CBF is measured by a phase-contrast (PC) quantitative flow technique applied at the feeding arteries at the base of the brain (Haccke et al., 1999). Phase-contrast MRI utilizes the phase of an image to encode the velocity of moving spins and has been validated for angiogram and quantitative flow measurements (Bakker et al., 1999; Evans et al., 1993; Zananiri et al., 1991). Y_a in Eq. [1] is measured with pulse oximetry.

MRI protocol—The pulse sequences and planning schemes for the $CMRO_2$ measurement were detailed previously (Liu et al., 2013). Briefly, we first performed an axial 3D time-of-flight (TOF) angiogram to visualize the brain's feeding arteries, internal carotid arteries (ICA) and vertebral arteries (VA). During the angiogram scan, the TRUST imaging slice was planned to be parallel to anterior-commissure posterior-commissure line with a distance of 20mm from the sinus confluence where the superior sagittal sinus (SSS), straight sinus and transverse sinus join (Figure 2A). This positioning scheme was previously shown to provide robust estimation of Y_v (Liu et al., 2013). While the TRUST scan was performed, four PC MRI scans were planned with the slices placed perpendicular to each of the left/right ICA and left/right VA arteries, providing an estimation of CBF (Figure 2C). The (one) TRUST and (four) PC scans provide a complete data set for $CMRO_2$ estimation. The

TRUST and PC MRI were repeated another eight times to obtain a time course of $CMRO_2$. An additional TRUST scan was performed at the end of the session. This allowed us to average between two consecutive TRUST scans to obtain an Y_v estimation that matches the acquisition time of PC MRI, which is important for accurate determination of $CMRO_2$.

Imaging parameters of the TRUST MRI were: TR = 3000ms, TI = 1022ms, voxel size = $3.44 \times 3.44 \times 5mm^3$, four different T_2-weightings with effective TE (eTE) of 1ms (gap between RF pulses < 0.6ms, as short as attainable), 40ms, 80ms and 160ms, with a τ_{CPMG} = 10ms, scan duration = 1.2min. PC MRI used: single slice, voxel size = $0.45 \times 0.45 \times 5mm^3$, FOV = $230 \times 230 \times 5mm^3$, maximum velocity encoding = 80cm/s, 4 averages, scan duration of one PC MRI scan was 0.5 minutes. Including scan preparation time, the time to collect each $CMRO_2$ data set is approximately 4.5 minutes.

A T_1-weighted magnetization-prepared rapid gradient-echo (MPRAGE) scan was also performed at the end of the MRI session to provide an estimation of brain volume.

Data analysis—Data processing of TRUST and PC MRI followed methods used previously (Lu and Ge, 2008; Lu et al., 2012; Xu et al., 2009). Briefly, for TRUST MRI data (Figure 2B), after motion correction and pair-wise subtraction between control and labeled images, a preliminary region-of-interest (ROI) was manually drawn to include the superior sagittal sinus. To further define the venous voxels, four voxels with the highest signals in the difference images in the ROI were chosen as the final mask for spatial averaging. The venous blood signals were then fitted to a monoexponential function to obtain T_2. The T_2 was in turn converted to Y_v via a calibration plot obtained by *in vitro* blood experiments under controlled oxygenation, temperature, and Hct conditions (Lu et al., 2012).

For each PC MRI data (Figure 2D), a ROI was manually drawn on the targeted artery based on the complex difference image. The operator was instructed to trace the boundary of the targeted artery without including adjacent vessels. The phase signals, i.e. velocity values, within the mask were summed to yield the blood flow of each artery. The sum of flow in all four arteries then yielded the total CBF to the brain (in ml/min) without accounting for brain volume. To obtain unit volume CBF values, the total flow was normalized to the parenchyma volume (i.e. gray matter + white matter), which was obtained from tissue segmentation (FSL software, FMRIB Software Library, Oxford University, UK) of the high-resolution T_1 image. Finally, the CBF value was divided by the tissue density of 1.06 g/ml (Herscovitch and Raichle, 1985), resulting in CBF in units of ml/100 g/min. $CMRO_2$ was calculated from Y_v, Y_a, CBF, and Hct using Eq. [1].

For statistical analysis, the physiological parameters (i.e. $CMRO_2$, CBF, Y_v, and OEF) measured under baseline (first time point) were compared to those at last time point using a mixed-effect model that utilizes both caffeine and control group data. This model investigates parametric changes over time within each group as well as the differences of the rate of changes between groups. By assuming that the caffeine-induced changes are linear with time, the analyses were repeated using all time points. Difference between caffeine and control groups was tested using two-sample t test. A Bonferroni corrected $p < 0.05$ is considered a significant effect.

Study 2: Regional heterogeneity of the caffeine effect on CBF

Experimental procedures—Ten healthy subjects (27±3 years old, range from 23 to 30, 4 males and 6 females) participated in this Study. The procedures were identical to the caffeine ingestion experiment in Study 1 except that the MRI pulse sequence used was a pseudo-continuous ASL (PCASL) sequence (Figure 1).

The PCASL pulse sequence used 3D GRASE acquisition with voxel size = $4 \times 4 \times 5mm^3$, shot TR = 3803ms, SENSE factor = 1.5/1.1 (RL/AP), four shots, volume TR=15 sec. Labeling parameters were: label duration (τ) = 1650ms, label delay = 1525ms, with background suppression. PCASL was continuously performed for 80 pairs of labeled and control images, resulting in a total PCASL scan duration of ~40 min.

Data analysis—The PCASL data were processed using in-house MATLAB (Mathworks, Natick, MA) scripts and the software SPM8 (University College London, UK). The processing steps included realignment, subtraction between each pair of control and labeled scans to obtain CBF weighted images, normalization of the images into MNI standard space, and quantification of CBF using a single compartment kinetic model (Alsop et al., 2014). By averaging two consecutive CBF maps to improve reliability, this dataset results in 40 dynamic CBF maps at 1 min temporal resolution.

Region-of-interest (ROI) analysis was conducted to compare the slower or faster CBF reduction (with time) between grey and white matter. A T_1-weighted high-resolution image was segmented using FSL (FSL software, FMRIB Software Library, Oxford, UK) to generate grey and white tissue masks for each individual, which were applied to the corresponding CBF maps to obtain CBF of each tissue type. Regression analysis was performed between CBF and time to compute a rate of reduction in % per minute. A paired Student t test was performed to compare the rate between grey and white matter.

Voxel-wise analysis was conducted to examine whether certain parts of the brain show faster or slower rate of CBF reduction than others. Only grey matter voxels were studied in this analysis because voxel-wise CBF value in the white matter is deemed unreliable. For each voxel inside the grey matter mask, we normalized its CBF value by the global grey matter CBF of the same time point, thereby factoring out the global CBF effect and providing a relative CBF (rCBF) map at each time point. We then conducted a voxel-by-voxel mixed-effect analysis, in which rCBF was the dependent variable while time was the fixed-effect independent variable and subject was the random-effect independent variable. Voxels with a positive (i.e. rCBF increases with time) or negative (i.e. rCBF decreases with time) time dependence were identified using a family-wise error (FWE) controlled p value less than 0.005 and cluster size larger than 100 voxels.

Results

Study 1

Figures 2B and D show representative images from the TRUST and PC MRI scans, respectively. No difference was found between the caffeine and control groups for $CMRO_2$, CBF or OEF at baseline (at the first time point, Table 1) using two-sample t test ($p>0.05$ for

all variables). Other baseline parameters such as Y_a and Hct were also comparable between the two groups. Y_a were 98.6±0.4 % and 98.5±0.3 % (p=0.88) for the caffeine and control groups, respectively. Hct were 42.2±1.0% and 39.9±1.5% (p=0.23), respectively.

Ingestion of caffeine tablet increased blood caffeine concentration. The blood test showed that caffeine concentration was 2.0±1.3mg/L at 1-hour after ingestion, consistent with expected values at this dosage (Kamimori et al., 2002). Table 1 shows the values of $CMRO_2$, CBF, Y_v, and OEF at the first (7 min after taking caffeine tablet) and last (~40 min after taking caffeine tablet) time points of the MRI session. The control group data are also shown. Mixed-effect analysis using both caffeine and control data revealed a significant time × group interaction for CBF ($p<0.001$), Y_v ($p=0.002$), and OEF ($p=0.002$), but not for $CMRO_2$ ($p=0.99$). For the caffeine group, global CBF decreased by 16.4% while OEF increased by 18.6%. Therefore, collectively, global $CMRO_2$ was found to be unchanged.

Time courses of all nine points are shown in Figure 3. All parameters have been normalized to their respective first time point. It can be seen that global CBF, Y_v and OEF were significantly altered by caffeine ingestion (Figure 3, red curves) while no changes were present in the control group (Figure 3, black curves). Under the assumption that the changes are linear with time, mixed-effect analysis was performed. The results revealed a significant time × group interaction for CBF ($p<0.001$), Y_v ($p<0.001$), and OEF ($p<0.001$), but not for $CMRO_2$ ($p=0.94$), similar to the two-point analysis results.

Study 2

Figures 4A and B show absolute CBF maps (averaged over 10 subjects) during the first and last minute of the ASL scan, respectively. It can be seen that CBF manifested a reduction across the entire brain. The rate of CBF decrease (in ml/min/100g per minute) is shown in Figure 4C. ROI analysis revealed that, in the grey matter, the rate of CBF reduction was 0.29±0.03 ml/min/100g per minute in absolute units and 0.50±0.05% per minute when using percentage units. In the white matter, the rate was 0.23±0.03 ml/min/100g per minute in absolute units and 0.58±0.07% per minute in percentage units. The white matter had a slightly faster rate of decline (in percentage units) compared to the gray matter, but this difference did not reach a significant level (p=0.09, two-tailed paired t test).

Voxel-wise analysis of the relationship between rCBF (normalized to the whole-brain grey matter CBF) and time revealed that some brain regions showed a significant time-dependent increase in rCBF (Figure 5A) while other regions showed a decrease (Figure 5B). As mentioned, a positive rCBF slope means that absolute CBF in these regions decreased slower than the whole-brain value. A negative rCBF slope means that absolute CBF decreased faster than the whole-brain value. Table 2 lists the anatomical locations of these clusters. It can be seen that the positive clusters (Figure 5A) are largely distributed in the posterior regions including nodes of the default-mode-network (DMN) such as posterior cingulate cortex and superior temporal region. In contrast, the negative clusters (Figure 5B) are mainly located in the anterior regions such as the dorsolateral prefrontal cortex and medial frontal cortex.

Discussion

The present study investigated the effect of acute caffeine ingestion on several physiological parameters including CBF, Y_v, OEF, and $CMRO_2$. Our data suggest that, following 200mg caffeine ingestion, whole-brain CBF decreased substantially while $CMRO_2$ did not show a change. As a result, the brain had to increase its OEF to obtain the same amount of total oxygen. The control group showed no effect of time on any of the four parameters, suggesting that the changes observed in the caffeine ingestion data were not due to subject becoming drowsy after being inside the MRI for a while. A further investigation using regional CBF measurement revealed that there exists some regional heterogeneity in the rate of decline. Specifically, posterior brain regions including posterior cingulate cortex and superior temporal region showed a slower CBF decline compared to anterior brain regions such as the dorsolateral prefrontal cortex and medial frontal cortex. Collectively, these data suggest that acute caffeine ingestion does not alter total brain oxygen consumption, but there could be regional heterogeneity in neural and/or vascular responses.

Physiological considerations

Pharmacologic effects of caffeine on the brain are numerous. Aside from the most well-known role of adenosine antagonist, this drug also has profound effects on several other neurotransmission systems including dopamine, acetylcholine, serotonin, norepinephrine, and GABA (Ferre, 2010; Fredholm et al., 1999; Nehlig et al., 1992). Its action on the adenosine system can be further divided based on subtypes of adenosine receptors and their distributions in the brain. An additional component of the complexity is that caffeine also has a strong constriction effect on vasculature itself (Chen and Parrish, 2009; Griffeth et al., 2011; Laurienti et al., 2002; Liu et al., 2004), thereby complicating the interpretation of vascular-based functional brain imaging results. Therefore, the exact effect of caffeine ingestion on the human brain is not fully elucidated to date and existing reports in the literature are discrepant with respect to one another. Based on the notion that adenosine is an inhibitory neuromodulator, the blockage of this effect by caffeine should therefore enhance neural activity. However, studies using electroencephalogram (EEG), magnetoencephalogram (MEG), and functional connectivity MRI have revealed a decrease in neural activity (Dimpfel et al., 1993; Siepmann and Kirch, 2002; Tal et al., 2013; Wong et al., 2012). Since neural activity is tightly coupled to energy consumption, brain metabolic rate would provide a useful surrogate marker of brain activity. Unfortunately, the vast majority of PET studies of caffeine only measured relative but not absolute values of metabolic rate of glucose, due to the absence of arterial sampling data (Di et al., 2013; Park et al., 2014; Specterman et al., 2005). Thus, the effect of caffeine ingestion on absolute metabolic rate could not be addressed in those studies.

The present study provided important evidence that whole-brain $CMRO_2$ did not change after caffeine, despite pronounced alterations in CBF and OEF. This is not congruent with the previous findings using EEG and MEG techniques (Dimpfel et al., 1993; Siepmann and Kirch, 2002; Tal et al., 2013). One possibility is that EEG and MEG reflect the synchrony of synaptic neural potentials, which could be different from the total energy expenditure of the brain that includes not only synaptic potentials but also action potentials and basal cellular

processes (Attwell and Laughlin, 2001). Another possibility is that there may be regional heterogeneities in caffeine response and that enhancement in some regions or suppression in others may result in an unchanged whole-brain metabolic rate.

Our second study examined regional changes in CBF, in reference to whole-brain CBF changes. We found that different brain regions manifested different rates of CBF reduction. Most notably, posterior brain regions such as posterior cingulate cortex and superior temporal region showed an increase in rCBF, i.e. absolute CBF value declines at a rate slower than the whole-brain grey matter (Figure 5). In contrast, anterior regions showed a decrease in rCBF.

There could be a few possible explanations for these observations. One is that caffeine may cause a neural enhancement in certain brain regions but suppression in others. Posterior cingulate cortex and superior temporal region are nodes of the DMN, which have been postulated to be related to consciousness and self-awareness (Raichle et al., 2001; Vago and Silbersweig, 2012) that may be associated with the effect of caffeine on vigilance. Other studies have also suggested that posterior regions may have elevated neural activity due to caffeine use. For example, a study of chronic caffeine overuse on brain migraine patients reported increased glucose metabolism in middle temporal gyrus (Di et al., 2013). Griffeth et al. used calibrated fMRI methods and showed a 20% increase in $CMRO_2$ in the visual cortex (Griffeth et al., 2011). Reduced regional activity has been noted in the literature (Park et al., 2014). A second possible explanation is that caffeine may have a region-dependent vascular effect and that the rCBF patterns observed reflect the spatial distribution of the corresponding adenosine receptors. Vascular effects of caffeine are primarily mediated by A_{2A} adenosine receptors (Pelligrino et al., 2010). Although the distribution of A_{2A} receptors in the brain has recently been examined using PET tracer methods (Mishina et al., 2007), the signal is expected to originate from both vascular and neuronal receptors. It was found that posterior regions had a slightly higher PET signal compared to frontal regions (Mishina et al., 2007). If vascular A_{2A} receptors were the primary source for this difference, one would expect that posterior regions should have a decrease in rCBF and anterior regions should have an increase. This is not congruent with the regional CBF results observed in the present study. Nonetheless, heterogeneity in direct vascular effects remains to be a potential explanation for our CBF findings. A third possibility is that the differences in ASL signal may reflect heterogeneity in vascular arrival time and their response to caffeine. A multi-delay ASL sequence can be used to separate the effects of CBF and arrival time changes (Gallichan and Jezzard, 2009).

The vasoconstriction effect of caffeine is well documented in the literature using PET, MRI, transcranial Doppler, and near infrared spectroscopy techniques (Addicott et al., 2009; Cameron et al., 1990; Kennedy and Haskell, 2011; Lunt et al., 2000; Lunt et al., 2004; Mathew and Wilson, 1985). Our findings of a CBF reduction using PC MRI and PCASL MRI are consistent with these prior reports and the amount of reduction is also within the expected range (15–25%).

Technical considerations

The present study used two MRI techniques to examine the effect of acute caffeine ingestion on brain activity. We first studied the effect of caffeine on whole-brain $CMRO_2$. The TRUST technique is a relatively new method developed in our laboratory (Lu and Ge, 2008; Lu et al., 2012; Xu et al., 2009) and we have previously shown that it has excellent test-retest reproducibility (Liu et al., 2013). The fact that it does not require any exogenous contrast agent allowed this technique to be applied dynamically in the same session, as was performed in the present study. However, it is important to point out that, in our calculation of global $CMRO_2$, we used blood flow measured at the global level but blood oxygenation level measured from the superior sagittal sinus. Superior sagittal sinus is a major vein of the brain but it drains only the cortical areas. Thus, our calculation is based on the assumption that Y_v measured in the superior sagittal sinus is a close approximation of the global Y_v. Our previous study has shown that Y_v in the sagittal sinus and jugular vein were comparable (Xu et al., 2009). Thus our assumption is likely valid in young, healthy controls as were examined in the present study. Nonetheless, it would have been ideal to measure Y_v directly in the jugular veins.

We found that caffeine ingestion did not alter global $CMRO_2$. An unchanged whole-brain $CMRO_2$ does not rule out any regional changes. Unfortunately, regional $CMRO_2$ techniques that can be used dynamically are not yet available. We therefore carried out another study in which CBF was used as a surrogate marker for metabolism. However, it should be noted that it is generally difficult to use vascular parameters as a marker to assess metabolic and neural activity in maneuvers that have a direct vasoactive effect, for example caffeine and breathing challenges. Therefore, further investigations with more direct measurement of regional neural/metabolic signal are needed to corroborate our findings.

Conclusion

The present study revealed that, despite a pronounced vascular effect of CBF reduction and OEF increase, whole-brain $CMRO_2$ did not alter significantly following the ingestion of a 200 mg caffeine tablet. However, assessment of regional CBF showed that the rate of its change was heterogeneous across brain areas, with the posterior regions showing a slower reduction compared to the anterior regions. These findings suggest that neural and/or vascular effects of caffeine are region-dependent.

Acknowledgments

The authors would like to express gratitude to Yamei Cheng, Salvador Pena and Rani Varghese for assistance with the experiments. This work was supported, in part, by the National Institutes of Health (R01 MH084021, R01 NS067015, R01 AG033106, R21 NS085634, and P41 EB15909).

References

Addicott MA, Yang LL, Peiffer AM, Burnett LR, Burdette JH, Chen MY, Hayasaka S, Kraft RA, Maldjian JA, Laurienti PJ. The effect of daily caffeine use on cerebral blood flow: How much caffeine can we tolerate? Hum Brain Mapp. 2009; 30:3102–3114. [PubMed: 19219847]

Alsop DC, Detre JA, Golay X, Gunther M, Hendrikse J, Hernandez-Garcia L, Lu H, Macintosh BJ, Parkes LM, Smits M, van Osch MJ, Wang DJ, Wong EC, Zaharchuk G. Recommended

implementation of arterial spin-labeled perfusion MRI for clinical applications: A consensus of the ISMRM perfusion study group and the European consortium for ASL in dementia. Magn Reson Med. 2014 Apr 8.10.1002/mrm.25197

Attwell D, Laughlin SB. An energy budget for signaling in the grey matter of the brain. J Cereb Blood Flow Metab. 2001; 21:1133–1145. [PubMed: 11598490]

Bakker CJ, Hoogeveen RM, Viergever MA. Construction of a protocol for measuring blood flow by two-dimensional phase-contrast MRA. J Magn Reson Imaging. 1999; 9:119–127. [PubMed: 10030659]

Berkowitz BA, Spector S. The effect of caffeine and theophylline on the disposition of brain serotonin in the rat. Eur J Pharmacol. 1971; 16:322–325. [PubMed: 5132559]

Berkowitz BA, Tarver JH, Spector S. Release of norepinephrine in the central nervous system by theophylline and caffeine. Eur J Pharmacol. 1970; 10:64–71. [PubMed: 5458986]

Cameron OG, Modell JG, Hariharan M. Caffeine and human cerebral blood flow: a positron emission tomography study. Life Sci. 1990; 47:1141–1146. [PubMed: 2122148]

Chen, Y.; Newberg, AB.; Wang, J.; Rao, H.; An, H.; Greenberg, J.; Wintering, N.; Toles, V.; Detre, JA. Caffeine's effects on resting-state oxygen and glucose metabolism: A combined MR and PET study. Proceedings of 17th annual meeting of international society for magnetic resonance in medicine; Hawaii, USA. 2009. p. 794

Chen Y, Parrish TB. Caffeine's effects on cerebrovascular reactivity and coupling between cerebral blood flow and oxygen metabolism. Neuroimage. 2009; 44:647–652. [PubMed: 19000770]

Di W, Shi X, Zhu Y, Tao Y, Qi W, Luo N, Xiao Z, Yi C, Miao J, Zhang A, Zhang X, Fang Y. Overuse of paracetamol caffeine aspirin powders affects cerebral glucose metabolism in chronic migraine patients. Eur J Neurol. 2013; 20:655–662. [PubMed: 23114018]

Dimpfel W, Schober F, Spuler M. The influence of caffeine on human EEG under resting conditions and during mental loads. Clin Investig. 1993; 71:197–207.

Donahue MJ, Lu H, Jones CK, Pekar JJ, van Zijl PC. An account of the discrepancy between MRI and PET cerebral blood flow measures. A high-field MRI investigation. NMR Biomed. 2006; 19:1043–1054. [PubMed: 16948114]

Evans AJ, Iwai F, Grist TA, Sostman HD, Hedlund LW, Spritzer CE, Negro-Vilar R, Beam CA, Pelc NJ. Magnetic resonance imaging of blood flow with a phase subtraction technique. In vitro and in vivo validation. Invest Radiol. 1993; 28:109–115. [PubMed: 8444566]

Ferre S. Role of the central ascending neurotransmitter systems in the psychostimulant effects of caffeine. J Alzheimers Dis. 2010; 20(Suppl 1):S35–49. [PubMed: 20182056]

Fredholm BB, Battig K, Holmen J, Nehlig A, Zvartau EE. Actions of caffeine in the brain with special reference to factors that contribute to its widespread use. Pharmacol Rev. 1999; 51:83–133. [PubMed: 10049999]

Gallichan D, Jezzard P. Variation in the shape of pulsed arterial spin labeling kinetic curves across the healthy human brain and its implications for CBF quantification. Magn Reson Med. 2009; 61:686–695. [PubMed: 19132757]

Golay X, Silvennoinen MJ, Zhou J, Clingman CS, Kauppinen RA, Pekar JJ, van Zijl PC. Measurement of tissue oxygen extraction ratios from venous blood T(2): increased precision and validation of principle. Magn Reson Med. 2001; 46:282–291. [PubMed: 11477631]

Goodman RR, Synder SH. Autoradiographic localization of adenosine receptors in rat brain using [3H]cyclohexyladenosine. J Neurosci. 1982; 2:1230–1241. [PubMed: 6288896]

Griffeth VE, Perthen JE, Buxton RB. Prospects for quantitative fMRI: investigating the effects of caffeine on baseline oxygen metabolism and the response to a visual stimulus in humans. Neuroimage. 2011; 57:809–816. [PubMed: 21586328]

Guyton, AC.; Hall, JE. Respiration. In: Guyton, AC.; Hall, JE., editors. Textbook of Medical Physiology. Saunders: Elsevier; 2005.

Haccke, EM.; Brown, RW.; Thompson, MR.; Venkatesan, R. Magnetic Resonance Imaging: Physical Principles and Sequence Design. Wiley-Liss; New York, NY: 1999. MR Angiography and Flow Quantification.

Herscovitch P, Raichle ME. What is the correct value for the brain--blood partition coefficient for water? J Cereb Blood Flow Metab. 1985; 5:65–69. [PubMed: 3871783]

Jain V, Langham MC, Wehrli FW. MRI estimation of global brain oxygen consumption rate. J Cereb Blood Flow Metab. 2010; 30:1598–1607. [PubMed: 20407465]

Kamimori GH, Karyekar CS, Otterstetter R, Cox DS, Balkin TJ, Belenky GL, Eddington ND. The rate of absorption and relative bioavailability of caffeine administered in chewing gum versus capsules to normal healthy volunteers. Int J Pharm. 2002; 234:159–167. [PubMed: 11839447]

Kennedy DO, Haskell CF. Cerebral blood flow and behavioural effects of caffeine in habitual and non-habitual consumers of caffeine: a near infrared spectroscopy study. Biol Psychol. 2011; 86:298–306. [PubMed: 21262317]

Kety SS, Schmidt CF. The Effects of Altered Arterial Tensions of Carbon Dioxide and Oxygen on Cerebral Blood Flow and Cerebral Oxygen Consumption of Normal Young Men. J Clin Invest. 1948; 27:484–492. [PubMed: 16695569]

Laurienti PJ, Field AS, Burdette JH, Maldjian JA, Yen YF, Moody DM. Dietary caffeine consumption modulates fMRI measures. Neuroimage. 2002; 17:751–757. [PubMed: 12377150]

Liu P, Xu F, Lu H. Test-retest reproducibility of a rapid method to measure brain oxygen metabolism. Magn Reson Med. 2013; 69:675–681. [PubMed: 22517498]

Liu TT, Behzadi Y, Restom K, Uludag K, Lu K, Buracas GT, Dubowitz DJ, Buxton RB. Caffeine alters the temporal dynamics of the visual BOLD response. Neuroimage. 2004; 23:1402–1413. [PubMed: 15589104]

Lu H, Ge Y. Quantitative evaluation of oxygenation in venous vessels using T2-Relaxation-Under-Spin-Tagging MRI. Magn Reson Med. 2008; 60:357–363. [PubMed: 18666116]

Lu H, Xu F, Grgac K, Liu P, Qin Q, van Zijl P. Calibration and validation of TRUST MRI for the estimation of cerebral blood oxygenation. Magn Reson Med. 2012; 67:42–49. [PubMed: 21590721]

Lunt MJ, Jenkinson DF, Kerr D. Transcranial Doppler blood velocity measurement--the effect of changes in velocity profile. Ultrasound Med Biol. 2000; 26:1145–1151. [PubMed: 11053749]

Lunt MJ, Ragab S, Birch AA, Schley D, Jenkinson DF. Comparison of caffeine-induced changes in cerebral blood flow and middle cerebral artery blood velocity shows that caffeine reduces middle cerebral artery diameter. Physiol Meas. 2004; 25:467–474. [PubMed: 15132312]

Magill RA, Waters WF, Bray GA, Volaufova J, Smith SR, Lieberman HR, McNevin N, Ryan DH. Effects of tyrosine, phentermine, caffeine Damphetamine, and placebo on cognitive and motor performance deficits during sleep deprivation. Nutr Neurosci. 2003; 6:237–246. [PubMed: 12887140]

Mathew RJ, Wilson WH. Caffeine induced changes in cerebral circulation. Stroke. 1985; 16:814–817. [PubMed: 3901422]

Mishina M, Ishiwata K, Kimura Y, Naganawa M, Oda K, Kobayashi S, Katayama Y, Ishii K. Evaluation of distribution of adenosine A2A receptors in normal human brain measured with [11C]TMSX PET. Synapse. 2007; 61:778–784. [PubMed: 17568431]

Nehlig A, Daval JL, Debry G. Caffeine and the central nervous system: mechanisms of action, biochemical, metabolic and psychostimulant effects. Brain Res Brain Res Rev. 1992; 17:139–170. [PubMed: 1356551]

Oja JM, Gillen JS, Kauppinen RA, Kraut M, van Zijl PC. Determination of oxygen extraction ratios by magnetic resonance imaging. J Cereb Blood Flow Metab. 1999; 19:1289–1295. [PubMed: 10598932]

Park CA, Kang CK, Son YD, Choi EJ, Kim SH, Oh ST, Kim YB, Park CW, Cho ZH. The effects of caffeine ingestion on cortical areas: functional imaging study. Magn Reson Imaging. 2014; 32:366–371. [PubMed: 24512799]

Pelligrino DA, Xu HL, Vetri F. Caffeine and the control of cerebral hemodynamics. J Alzheimers Dis. 2010; 20(Suppl 1):S51–62. [PubMed: 20182032]

Premont J, Perez M, Blanc G, Tassin JP, Thierry AM, Herve D, Bockaert J. Adenosine-sensitive adenylate cyclase in rat brain homogenates: kinetic characteristics, specificity, topographical, subcellular and cellular distribution. Mol Pharmacol. 1979; 16:790–804. [PubMed: 530259]

Raichle ME, MacLeod AM, Snyder AZ, Powers WJ, Gusnard DA, Shulman GL. A default mode of brain function. Proc Natl Acad Sci U S A. 2001; 98:676–682. [PubMed: 11209064]

Rodgers ZB, Jain V, Englund EK, Langham MC, Wehrli FW. High temporal resolution MRI quantification of global cerebral metabolic rate of oxygen consumption in response to apneic challenge. J Cereb Blood Flow Metab. 2013; 33:1514–1522. [PubMed: 23838827]

Siepmann M, Kirch W. Effects of caffeine on topographic quantitative EEG. Neuropsychobiology. 2002; 45:161–166. [PubMed: 11979068]

Silvennoinen MJ, Clingman CS, Golay X, Kauppinen RA, van Zijl PC. Comparison of the dependence of blood R2 and R2* on oxygen saturation at 1.5 and 4.7 Tesla. Magn Reson Med. 2003; 49:47–60. [PubMed: 12509819]

Specterman M, Bhuiya A, Kuppuswamy A, Strutton PH, Catley M, Davey NJ. The effect of an energy drink containing glucose and caffeine on human corticospinal excitability. Physiol Behav. 2005; 83:723–728. [PubMed: 15639157]

Tal O, Diwakar M, Wong CW, Olafsson V, Lee R, Huang MX, Liu TT. Caffeine-Induced Global Reductions in Resting-State BOLD Connectivity Reflect Widespread Decreases in MEG Connectivity. Front Hum Neurosci. 2013; 7:63. [PubMed: 23459778]

Vago DR, Silbersweig DA. Self-awareness, self-regulation, and self-transcendence (S-ART): a framework for understanding the neurobiological mechanisms of mindfulness. Front Hum Neurosci. 2012; 6:296. [PubMed: 23112770]

Wong CW, Olafsson V, Tal O, Liu TT. Anti-correlated networks, global signal regression, and the effects of caffeine in resting-state functional MRI. Neuroimage. 2012; 63:356–364. [PubMed: 22743194]

Xu F, Ge Y, Lu H. Noninvasive quantification of whole-brain cerebral metabolic rate of oxygen (CMRO2) by MRI. Magn Reson Med. 2009; 62:141–148. [PubMed: 19353674]

Xu F, Uh J, Liu P, Lu H. On improving the speed and reliability of T(2) - relaxation-under-spin-tagging (TRUST) MRI. Magn Reson Med. 2011

Zananiri FV, Jackson PC, Goddard PR, Davies ER, Wells PN. An evaluation of the accuracy of flow measurements using magnetic resonance imaging (MRI). J Med Eng Technol. 1991; 15:170–176. [PubMed: 1800748]

Highlights

- CBF decreases with caffeine ingestion while oxygen extraction fraction increases.
- Global CMRO2 does not change with caffeine ingestion
- There exists regional heterogeneity in the rate of CBF reduction
- Effect of caffeine on neuron and/or vasculature appears to be region-dependent

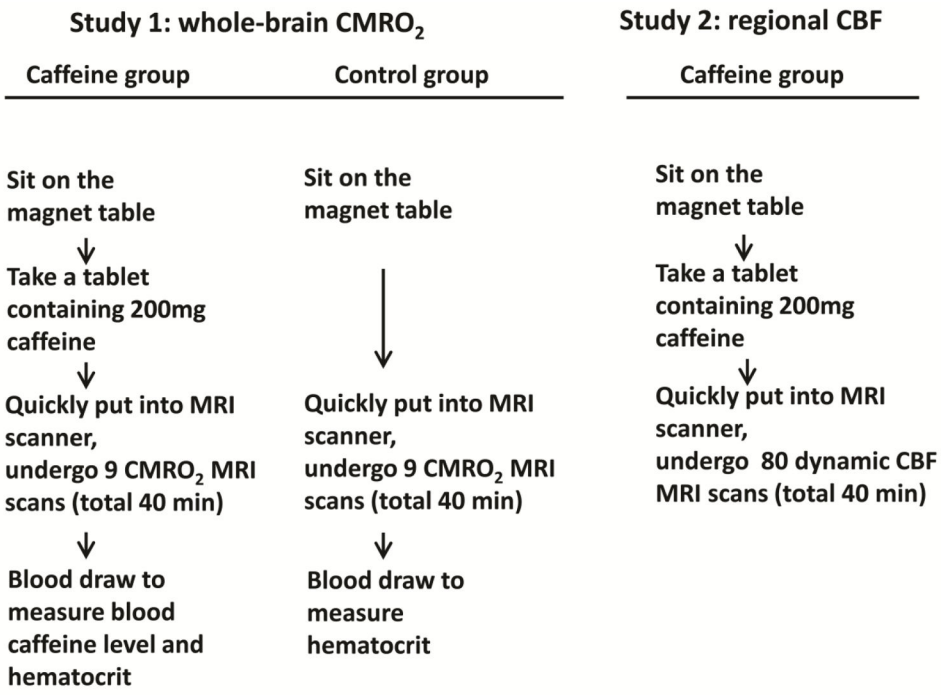

Figure 1.

Diagram of experimental procedures used in Study 1 and Study 2. Study 1 (left) contained a group of caffeine ingestion and a group of control participants. Study 2 (right) was performed on a caffeine ingestion group only as Study 1 already demonstrated that CBF does not change under the control condition.

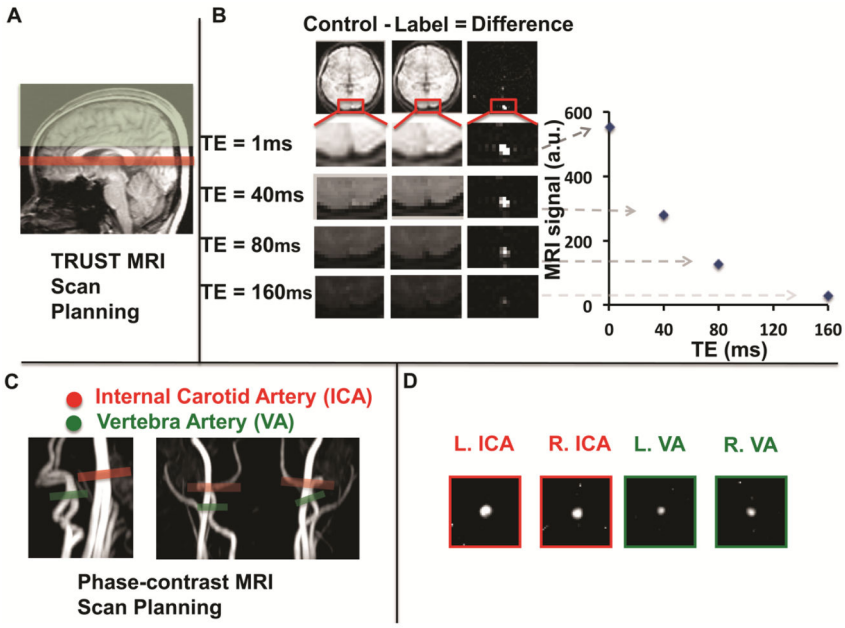

Figure 2.

Slice positioning and representative image data of MRI scans performed for the whole brain $CMRO_2$ estimation. (A) Imaging planning of T_2-Relaxation-Under-Spin-Tagging (TRUST) MRI for the measurement of global venous oxygenation. Red area: imaging slice. Green area: labeling slab. (B) Representative control and labeled images from TRUST MRI as well as their difference. The area containing the superior sagittal sinus is amplified in the red box. Control and labeled images were acquired at four effective TEs. The plot on the right shows the difference signal in the superior sagittal sinus as a function of effective TE. (C) Imaging planning of Phase-Contrast (PC) MRI. The background images are sagittal and coronal views of the time-of-flight angiogram showing the internal carotid and vertebral arteries. Four PC MRI scans were performed, each placed perpendicular to a targeted artery. Red bars: slices intersecting left/right internal carotid arteries at level of foreman magnum where arteries enter the skull. Green bars: slices intersecting vertebral arteries. They are placed slightly outside the skull, in order to achieve a perpendicular angle. (D) Representative complex difference images from PC MRI. For convenience, only the portion that contains the targeted vessel is shown.

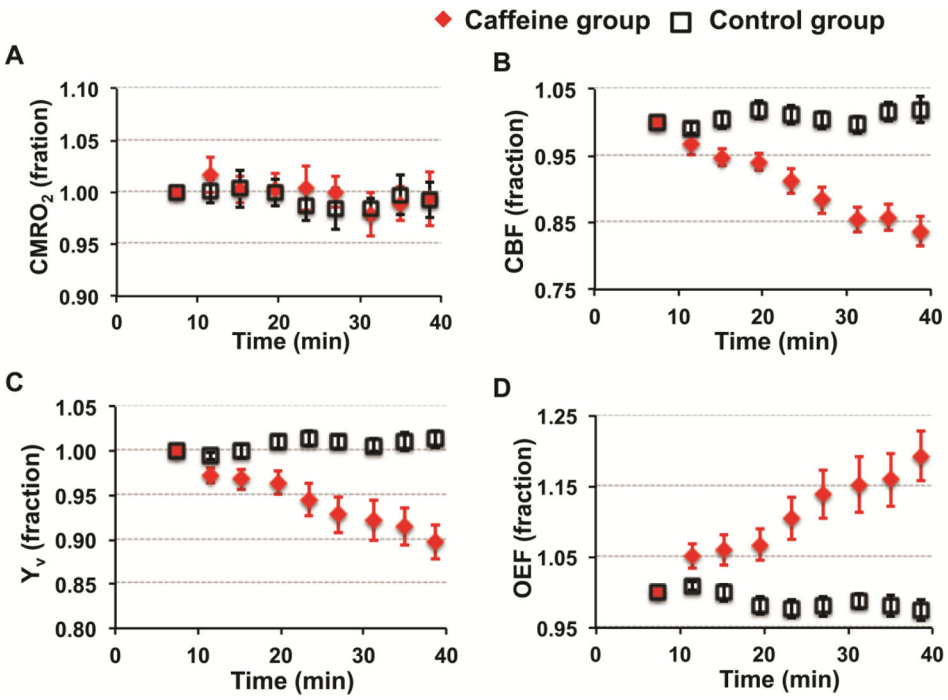

Figure 3.

Time courses of relative changes in (A) $CMRO_2$, (B) CBF, (C) Y_v, and (D) OEF. The y-axis values were normalized against the values of the first time point on an individual basis. Thus they are shown in fractions and the first time point does not have an error bar. Red dots are the data from the caffeine ingestion group (mean±SE), while black dots are data from the control group. Time point "0" indicates the time of caffeine ingestion for the caffeine group and the time of the subject entering the scanner for the control group.

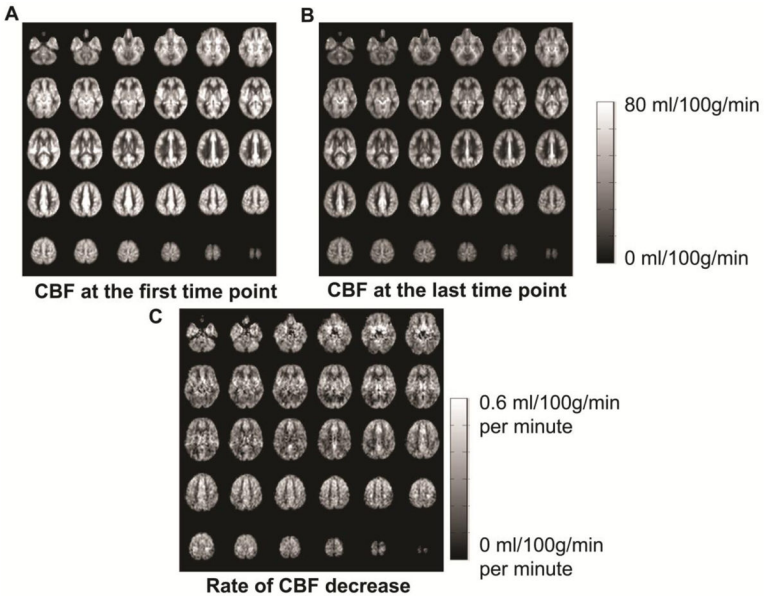

Figure 4.

Absolute CBF maps (averaged over 10 subjects, in ml/min^{2}100g) at (A) the first time point and (B) the last time point of the ASL scan. (C) Rate of absolute CBF change with time (in ml/100g/min per minute. The rate was calculated with a voxel-wise mixed linear model using data from all 10 subjects.

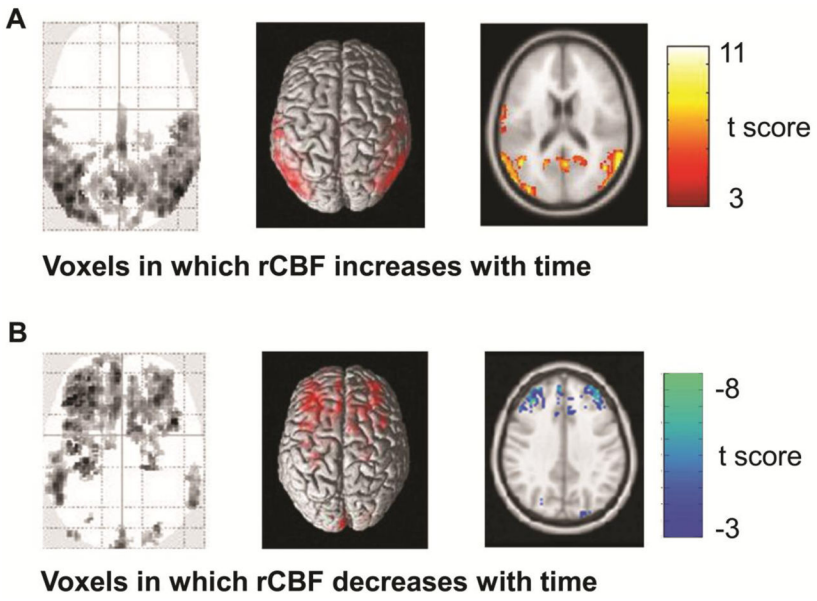

Figure 5.

Voxels with a time-dependent change in *relative* CBF (rCBF). rCBF was calculated by dividing the individual voxel's absolute CBF value by the whole-brain averaged value of the same time point. (A) Regions in which rCBF increases with time, suggesting a slower rate of CBF reduction compared to the global CBF. (B) Regions in which rCBF decreases with time, suggesting a faster rate of CBF reduction compared to the global CBF. Thresholds: $p<0.005$ and cluster size>100. The maps are shown in axial glass (left), rendered (middle) and sectional (right) views.

Table 1

Physiological parameters at the first time point (i.e. ~7 min after caffeine ingestion) and the last time point (i.e. ~40 min after caffeine ingestion) of the MRI session. Values are listed in mean ± standard error.

Condition	$CMRO_2$ (μmol/100g/min)	CBF (ml/100g/min)	Y_v (%)	OEF (%)
	Caffeine ingestion group			
The first time point	164.0±7.4	57.8±2.0	62.8±1.7	36.3±1.8
The last (9^{th}) time point	162.6±5.4	48.4±1.5	56.1±1.6	42.8±1.8
	Control group			
The first time point	167.6±6.5	58.1±2.7	59.8±1.3	39.3±1.4
The last (9^{th}) time point	166.7±6.2	58.0±2.8	59.6±2.1	39.5±2.1

Table 2

List of clusters with a CBF reduction rate significantly different from the whole-brain value. Panel A lists the clusters by peak voxel location. Panel B lists the clusters by fractions of voxels in major anatomic regions. Matrix indices are the x, y, z coordinates in the image matrix with a dimension of 91 × 109 × 91. MNI coordinate is the location away from origin in directions of left-right (LR), posterior-anterior (PA) and foot-head (FH).

Panel A

Cluster index	Matrix index (X, Y, Z)	MNI coordinate (LR, PA, FH)	Location of the peak voxel in the cluster	Cluster size (ml)	Brodmann area
	Slower (positive rCBF slope) CBF reduction				
1	36, 32, 42	−20, −64, 10	Posterior cingulate cortex	19.4	23
2	47, 66, 51	2, 4, 28	Cingulate gyrus	5.0	7
3	72, 29, 51	52, −70, 28	Middle temporal gyrus	25.5	40
4	27, 19, 45	−38, −90, 16	Middle occipital gyrus	32.7	31
5	44, 30, 52	−4, −68, 30	Cuneus	1.0	19
	Faster (negative rCBF slope) CBF reduction				
1	44, 57, 72	−4, −14, 70	Medial frontal gyrus	2.0	6
2	60, 81, 55	28, 34, 36	Superior frontal gyrus	40.8	9
3	48, 17, 44	4, −94, 14	Cuneus	1.9	18
4	57, 21, 52	22, −86, 30	Cuneus	0.67	19
5	21, 36, 26	−50, −56, −22	Temporal fusiform gyrus	4.2	37, 20
6	76, 45, 27	60, −38, −20	Inferior temporal gyrus	1.7	37, 20

Panel B

Cluster index	Anatomic regions (% of voxels)
	Slower (positive rCBF slope) CBF reduction
1	Left and right: posterior cingulate (13.0%); superior occipital (5.0%); lingual gyrus (20.1%), cuneus (5.2%); inferior occipital (5%); fusiform 26.7%, precuneus (4.2%,)
2	Left and Right: dorsal segment anterior cingulate (50.1%); posterior cingulate (26.5%); parietal (20.4%); temporal (2.7%)
3	Right: parietal (48.6%); superior temporal (9.7%); middle temporal (12.1%); middle occipital (10.9%); inferior occipital (3.4%)
4	Left: inferior occipital (6.4%); middle occipital (17.7%); fusiform (14.1%); middle temporal (13.1%); parietal (39.3%); superior occipital (1.4%); superior temporal (1.4%)
5	Left: precuneus (78.2%); occipital (11.3%); posterior cingular cortex (8.1%)
	Faster (negative rCBF slope) CBF reduction
1	Left: precentral gyrus (42%); postcentral gyrus (35.6 %); posterior segment of superior prefrontal gyrus (22.3%)

Panel B

Cluster index	Anatomic regions (% of voxels)
2	Left and right: superior frontal gyrus (46.2%); middle frontal gyrus (41.8%); anterior cingulate (5.5%); precentral gyrus (4.3%); gyrus rectus (1.7%)
3	Left and right: cuneus (100%)
4	Right: middle occipital (86.9%); superior occipital (13.1%)
5	Left: inferior temporal gyrus (86.1%); fusiform (2.64%); middle temporal gyrus (8.5%)
6	Right: inferior temporal gyrus (72.5%); middle temporal gyrus (11.7%); superior occipital (1.4%); inferior occipital (3.3%); fusiform (0.5%)